Kidney Stone Imaging with 3D Ultra-Short Echo Time (UTE) Magnetic Resonance Imaging. A Phantom Study

El-Sayed H. Ibrahim, Robert A. Pooley, Mellena D. Bridges, Joseph G. Cernigliaro, William E. Haley

Abstract— **Computed tomography (CT) is the current gold standard for imaging kidney stones, albeit at the cost of radiation exposure. Conventional magnetic resonance imaging (MRI) sequences are insensitive to detecting the stones because of their appearance as a signal void. With the development of 2D ultra-short echo-time (UTE) MRI sequences, it becomes possible to image kidney stones in vitro. In this work, we optimize and implement a modified 3D UTE MRI sequence for imaging kidney stones embedded in agarose phantoms mimicking the kidney tissue and in urine phantoms at 3.0T. The proposed technique is capable of imaging the stones with high spatial resolution in a short scan time.**

I. Introduction

Nephrolithiasis is a common chronic kidney disease, second only to hypertension. Approximately 11% of men and 7% of women will have a kidney stone event in their lives and these numbers appear to be increasing [1]. Many of these patients are likely to be repeated stone formers with 40% likelihood of developing a second stone in 5 years [2].

Computed tomography (CT) has been established as the method of choice for kidney stone imaging with a 90-100% sensitivity [3]. Further, the recent introduction of dual-energy CT (DECT) scanners adds the capability of differentiating uric-acid (UA) from non-UA stones [4]. A drawback of CT scanning is the associated ionizing radiation exposure. A recent study of 1-year cumulative radiation exposure in patients presenting with an acute stone episode revealed a median dose of 29.7 mSv per patient [5]. Despite the development of low-dose protocols, there is a potential risk, particularly among those requiring multiple repeated exposures, and among children and women of childbearing potential. Further, the recently proposed low-dose protocols, which may reduce radiation dose by up to 75%, require advanced technology that has not been widely implemented.

Magnetic resonance imaging (MRI) is a potential alternative to CT. MRI has shown a huge potential for noninvasive evaluation of multiple parameters of renal function such as glomerular filtration, tubular concentration, regional perfusion, water movements, and oxygenation, as well as demonstrating secondary effects of renal obstruction [6,7]. Nevertheless, current MRI pulse sequences with conventional echo times (TE's) are insensitive for direct imaging of kidney stones due to the stones' very short T2 time constants. This results in the stones appearing as a non-specific signal void that can be confused with blood, gas, and tumors [8], although stone visibility is improved with larger stone size (> 1 cm) and the presence of high signal intensity from surrounding urine [9]. Consequently, MRI is not currently recommended for kidney stone imaging. Figure 1 shows two example of signal voids in MRI images, one representing a stone and the other due to imaging artifact.

With the advent of ultra-short echo time (UTE) MRI sequences, adequate imaging of kidney stones becomes possible [10]. The UTE sequence design allows for TE's in the range of tens of microseconds, which provides the opportunity for imaging tissues with rapid signal decay, such as kidney stones. Different structures including tendons, ligaments, cortical bone, and discs have been successfully imaged with UTE MRI without contrast enhancement [8]. UTE sequences use half excitation RF pulses combined with radial acquisition starting from the k-space center [8]. Rephasing the slice-selective RF pulse is avoided by collecting the data twice with the slice-selection gradient applied in opposite directions, which further reduces TE [11]. UTE MRI has the advantage that the k-space center is oversampled so that the signal-to-noise ratio (SNR) of the

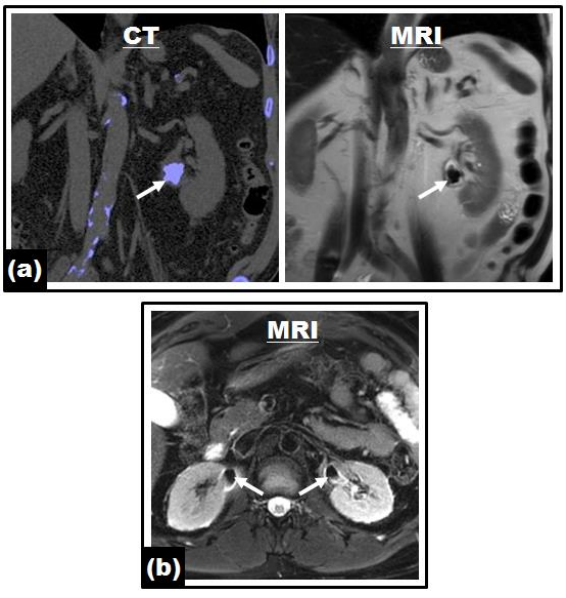

Figure 1. Conventional MRI images. (a) The MRI image on the right shows a good example of detecting kidney stone (arrow) compared to gold standard CT image on the left. (b) The signal voids are due to T2* artifact associated with concentrated gadolinium in the collecting system (arrows). These signal voids could be mistaken for stones.

E. H. Ibrahim (corresponding author) is with Mayo Clinic, Jacksonville, FL 32224, USA; phone: 904-953-6037; fax: 904-953-6581 (e-mail: ibrahim.elsayed@mayo.edu).

R. A. Pooley, M. D. Bridges, J. G. Cernigliaro, and W. E. Haley are with Mayo Clinic, Jacksonville, FL, USA (e-mails: pooley.robert@mayo.edu ; bridges.mellena@mayo.edu ; cernigliaro.joseph@mayo.edu ; haley.william@mayo.edu).

978-1-4244-7929-0/14/$26.00 ©2014 IEEE

low-frequency components in the image is higher than that of the high-frequency components, resulting in enhanced image contrast. However, UTE sequences are sensitive to delays in coil switching and eddy currents, which may produce a mottled effect on the resulting images.

Recently, Yassin et al [10] implemented a 2D UTE sequence on a 1.5T scanner to characterize the relaxation times of different kidney stones in vitro. The imaging sequence detected 58% of the stones with a size threshold of 0.9 cm for stone detection. Although an overlap existed between the relaxation times of stones with different compositions, the authors showed that the calcium phosphate (CaP) stones had longer T1 and T2 values than non-CaP stones. It should be noted that the performance of the UTE sequence in that study was not optimal due to the use of a 2D sequence on a 1.5T scanner, which resulted in relatively long scan time (> 5 min) and low sensitivity for stone detection.

The point-wise encoding time reduction with radial acquisition (PETRA) 3D UTE imaging sequence has recently been developed [12], leveraging the capabilities of 3D imaging for improving SNR and spatial resolution. In this study, we optimize and investigate the capability of the PETRA sequence for imaging kidney stones in vitro at 3.0T.

II. Methods

A. PETRA Pulse Sequence

In the PETRA pulse sequence, the outer k-space is filled with radial half-projections whereas the k-space center is measured point-wise on a Cartesian trajectory [12] (Figure 2). The single-point imaging with T1 enhancement (SPRITE) approach used in PETRA resolves the problems associated with conventional 2D UTE sequences by removing the delays associated with rapid gradients switching through turning on the imaging gradients prior to excitation [13]. Further, PETRA uses short RF excitation pulses with wide bandwidth to equally excite the whole volume regardless of the imaging gradient strength [11]. Compared to conventional 2D UTE sequences, PETRA provides much shorter TE over the whole k-space, which allows for better imaging of tissues with very short T2. Further, PETRA is less sensitive to eddy currents and gradient time delays than conventional 2D UTE sequences. In this study, kidney stones are imaged by acquiring two images with different TE's, which after subtraction eliminates the signal from long T2 tissues.

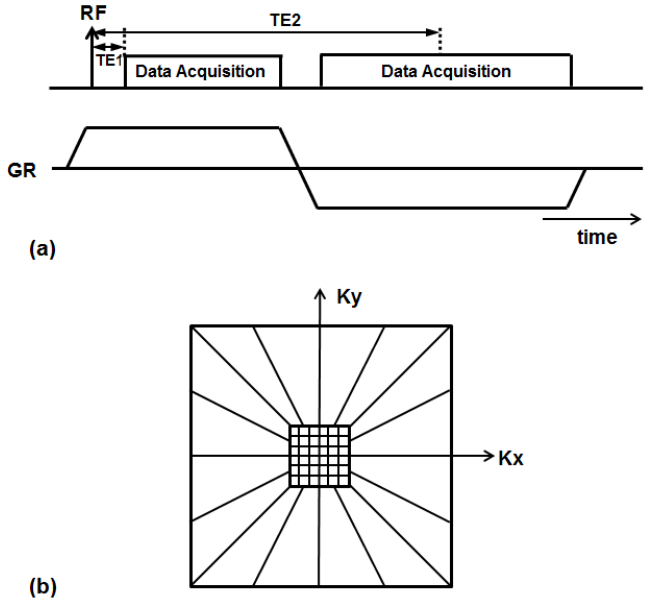

Figure 2. PETRA pulse sequence. (a) Radial acquisition of k-space periphery, where the gradients are ramped before RF excitation, which reduces TE compared to conventional UTE sequences. (b) k-space sampling, where the k-space center is acquired in Cartesian fashion.

B. Experiment Setup

Five 50-mL vials were filled with agarose-based material, created by dissolving 0.5% agarose in distilled water and doping the mixture with 0.085 milli-molar of MnCl2 to create a gel-like material with T1 and T2 values similar to those in the kidney (Figure 3) [14]. Eight kidney stones of different sizes and shapes were inserted inside the tubes when the gel-like material started to solidify. Table 1 lists the size and composition (as determined by infrared spectroscopy analysis conducted at Mayo Minerals Laboratory) of the different stones. Additional three vials were filled with urine and included six stones as shown in Figure 3 and Table 2.

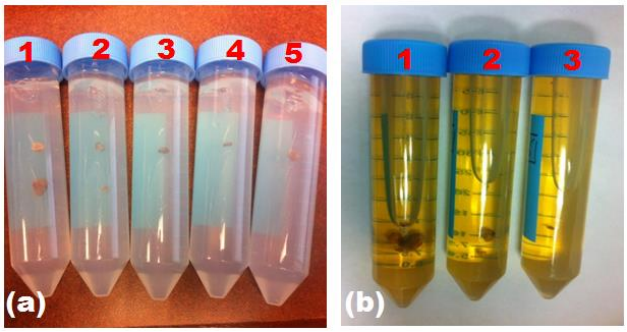

Figure 3. Phantoms. (a) Agarose phantoms. (b) Urine phantoms.

Table 1. Characterization of the imaged stones in the agarose phantoms.

Vial #	# Stones	Size (mm)	Composition	T2 (ms)
1	3	2, 5, 7	70% Uric Acid 30% Ca Ox monohydrate	5.2
2	2	3, 4	70% Brushite 20% Apatite 10% Ca Ox dihydrate	3.8
3	1	3	100% Ca Ox monohydrate	8.5
4	1	4	50% Ca Ox monohydrate 40% Ca Ox dihydrate 10% Apatite	6.8
5	1	4	80% Ca Ox monohydrate 10% Ca Ox dihydrate 10% Apatite	7.9

Table 2. Characterization of the imaged stones in the urine phantoms.

Vial #	# Stones	Size (mm)	Composition
1	3	1, 3, 6	70% Uric Acid 30% Ca Ox monohydrate
2	1	2	70% Brushite 20% Apatite 10% Ca Ox dihydrate
3	2	2, 5	100% Ca Ox monohydrate

C. Imaging Sequence and Image Reconstruction

The phantom was imaged using the 3D PETRA pulse sequence on a 3.0T MRI scanner (Siemens Skyra, Siemens Healthcare, Erlangen, Germany) using a commercial knee coil. The imaging parameters were as follows: flip angle = 6°; repetition time (TR) = 25 ms; first echo time (TE1) = 0.07 ms; second echo time (TE2) = 15 ms; slice thickness = 0.59 mm; field of view (FOV) = 150×150 mm^2; matrix = 256×256; number of radials = 2500; bandwidth = 1860 Hz/pixel; number of averages = 1; and scan time = 65 s. During image reconstruction, the longer TE image was automatically subtracted from the shorter TE image, which removed the signals from the background tissues and left only the signals from the stones. The imaging sequence was repeated for the agarose phantoms with different TE's ranging from 0.1 ms to 15 ms to measure T2 values of the stones. The images were transferred to a workstation provided by the scanner manufacturer, where 3D maximum intensity projection (MIP) reconstruction was conducted.

III. Results

Figures 4 and 5 show representative 2D cross-sectional and 3D MIP images (respectively) of the phantom. The imaging sequence successfully detected all the stones and showed them with high resolution, such that their shapes and surface topology can be identified, which were in agreement with visual inspection of the stones. The resulting images had very high spatial resolution, such that a sub-millimeter stone fraction was successfully detected in the image in Figure 4. The 3D images provided better information about the stones' shapes, orientations, and sizes, even for the smallest stone in the phantom (Fig. 5). No differences in the stones appearance were observed between the stones in the agarose and urine phantoms. The resulting T2 values ranged from 3.8 ms to 8.5 ms, as shown in Table 1, and specific ranges of T2 values varied with the stone compositions.

IV. Discussion

Computed tomography is the established modality of choice for imaging kidney stones due to its high sensitivity for stone detection, although this advantage comes at the cost of associated ionizing radiation exposure. MRI, with its high spatial resolution, superior tissue contrast, and lack of ionizing radiation, could be a potential alternative to CT for imaging kidney stones in vulnerable patients, e.g. children, pregnant women and those with childbearing potential, and

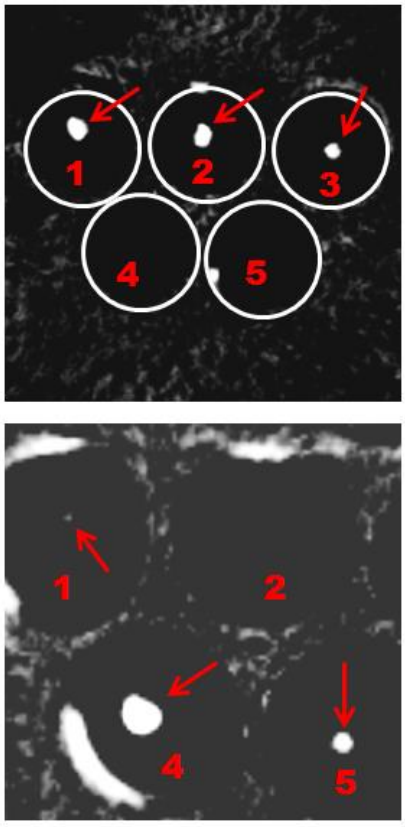

Figure 4. Phantom 2D images. Two-dimensional images showing cross-sections of the stones (arrows) inside the agarose phantoms. The image on the bottom shows a fraction from a stone in vial #1.

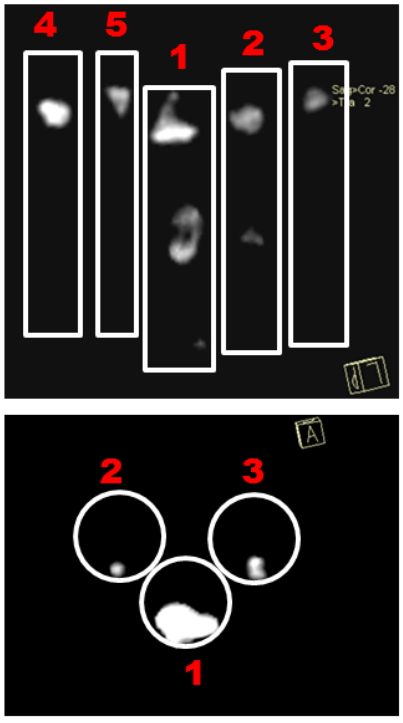

Figure 5. 3D MIP images. Three-dimensional maximum intensity projection (MIP) reconstruction showing the stones in the agarose (up) and urine (bottom) phantoms. The 3D images reveal the stones' shapes.

patients requiring multiple scans. However, conventional MRI sequences are insensitive for direct imaging of kidney stones, which appear as signal void and can be confused with other tissues or image artifacts. As a consequence, MRI is not currently recommended for imaging kidney stones. We found one article in the literature that examined the appearance of kidney stones in conventional MRI images and noted improved stone visibility for stone size >1 cm [9].

With the development of UTE MRI sequences, adequate imaging of kidney stones may become possible due to the achievable TE's in the order of microseconds, which allows for producing images with bright stones. We found one study that examined the implementation of a 2D UTE sequence for imaging kidney stones in vitro at 1.5T, with the results limited by long scan time and low sensitivity for stone detection [10]. In the present work, we addressed the limitations of imaging kidney stones with 2D UTE by adopting the advanced 3D UTE PETRA sequence for in vitro imaging of kidney stones at 3.0T. The imaging sequence was used to image stones of different sizes and compositions inside agarose and urine phantoms. The PETRA pulse sequence design as well as its 3D nature of data acquisition combined with imaging at 3.0T field strength allowed for detecting sub-millimeter stones in one fifth of the scan time used for 2D UTE imaging at 1.5T [10].

These preliminary results show the possibility of using PETRA for imaging kidney stones in vivo with high resolution in a short scan time. Future work includes imaging a large number of stones with different types to study the relationship between their T2 values and stone composition, compare the results to gold standard CT, and study test-retest reproducibility. Future work also includes a retrospective study of patients imaged with conventional MRI sequences to identify false positives that provide signal voids similar to the stones' appearance, as well as a prospective study to optimize the UTE sequence for in vivo imaging of patients with the phased-array coil, and addressing potential artifacts (e.g., flow, motion, off resonance from liver fat, and partial volume effects from large FOV). The developed technique could serve as an alternative technique for imaging vulnerable patients with concerns for radiation exposure. It could be also added to other abdomen / pelvis MRI protocols for comprehensive evaluation of the genitourinary system including scanning for stones.

V. Conclusions

The 3D PETRA UTE sequence is capable of imaging kidney stones in vitro with high resolution in a short scan time. With additional optimization for in vivo imaging, this sequence has a potential for in vivo imaging, particularly vulnerable patients including children, pregnant women, and stone formers requiring frequent imaging studies.

Acknowledgment

We acknowledge Siemens Healthcare for providing the PETRA imaging sequence used in this study.

References

[1] C. D. Scales, Jr., A. C. Smith, J. M. Hanley, and C. S. Saigal, "Prevalence of kidney stones in the United States," *European urology,* vol. 62, pp. 160-5, Jul 2012.

[2] E. M. Worcester and F. L. Coe, "Clinical practice. Calcium kidney stones," *The New England journal of medicine,* vol. 363, pp. 954-63, Sep 2 2010.

[3] I. Boulay, P. Holtz, W. D. Foley, B. White, and F. P. Begun, "Ureteral calculi: diagnostic efficacy of helical CT and implications for treatment of patients," *AJR. American journal of roentgenology,* vol. 172, pp. 1485-90, Jun 1999.

[4] D. T. Boll, N. A. Patil, E. K. Paulson, E. M. Merkle, W. N. Simmons, S. A. Pierre, and G. M. Preminger, "Renal stone assessment with dual-energy multidetector CT and advanced postprocessing techniques: improved characterization of renal stone composition--pilot study," *Radiology,* vol. 250, pp. 813-20, Mar 2009.

[5] M. N. Ferrandino, A. Bagrodia, S. A. Pierre, C. D. Scales, Jr., E. Rampersaud, M. S. Pearle, and G. M. Preminger, "Radiation exposure in the acute and short-term management of urolithiasis at 2 academic centers," *The Journal of urology,* vol. 181, pp. 668-72; # 673, 2009.

[6] N. Grenier, F. Basseau, M. Ries, B. Tyndal, R. Jones, and C. Moonen, "Functional MRI of the kidney," *Abdominal imaging,* vol. 28, pp. 164-75, Mar-Apr 2003.

[7] M. Budau, M. Onu, V. Jinga, B. Braticevici, and T. Pop, "US and MRI in renal obstruction evaluation," *Archivio italiano di urologia, andrologia : organo ufficiale [di] Societa italiana di ecografia urologica e nefrologica / Associazione ricerche in urologia,* vol. 74, pp. 59-60, Jun 2002.

[8] M. D. Robson, P. D. Gatehouse, M. Bydder, and G. M. Bydder, "Magnetic resonance: an introduction to ultrashort TE (UTE) imaging," *Journal of computer assisted tomography,* vol. 27, pp. 825-46, 2003.

[9] B. Kalb, P. Sharma, K. Salman, K. Ogan, J. G. Pattaras, and D. R. Martin, "Acute abdominal pain: is there a potential role for MRI in the setting of the emergency department in a patient with renal calculi?," *Journal of magnetic resonance imaging : JMRI,* vol. 32, pp. 1012-23, Nov 2010.

[10] A. Yassin, I. Pedrosa, M. Kearney, E. Genega, N. M. Rofsky, and R. E. Lenkinski, "In vitro MR imaging of renal stones with an ultra-short echo time magnetic resonance imaging sequence," *Academic radiology,* vol. 19, pp. 1566-72, Dec 2012.

[11] M. D. Robson and G. M. Bydder, "Clinical ultrashort echo time imaging of bone and other connective tissues," *NMR in biomedicine,* vol.19, pp. 765-80, 2006.

[12] D. M. Grodzki, P. M. Jakob, and B. Heismann, "Ultrashort echo time imaging using pointwise encoding time reduction with radial acquisition (PETRA)," *Magnetic resonance in medicine : official journal of the Society of Magnetic Resonance in Medicine,* vol. 67, pp. 510-8, Feb 2012.

[13] B. J. Balcom, R. P. Macgregor, S. D. Beyea, D. P. Green, R. L. Armstrong, and T. W. Bremner, "Single-Point Ramped Imaging with T1 Enhancement (SPRITE)," *Journal of magnetic resonance. Series A,* vol. 123, pp. 131-4, Nov 1996.

[14] S. H. Ibrahim el, F. N. Rana, K. R. Johnson, and R. D. White, "Assessment of cardiac iron deposition in sickle cell disease using 3.0 Tesla cardiovascular magnetic resonance," *Hemoglobin,* vol. 36, pp. 343-61, 2012.